PRECISION TEST OF THE SM WITH Kl2 AND Kl3 DECAYS AT KLOE

T. SPADARO
Laboratori Nazionali di Frascati dell'INFN, Via E. Fermi, 40,
00044 Frascati (Roma), Italy

Kaon decay studies seeking new-physics (NP) effects in leptonic (K_{l2}) or semileptonic (K_{l3}) decays are discussed. A unitarity test of the first row of the CKM mixing matrix is obtained from the KLOE precision measurements of Kl3 widths for $K^{\pm}$, K_L, and (unique to KLOE) K_S, complemented with the absolute branching ratio for the $K_{\mu 2}$ decay. KLOE results lead to constraints for NP models and can probe possible charged Higgs exchange contribution in SM extensions with two Higgs doublets. The main focus in the present document is set on a new measurement of $R_K = \Gamma(K_{e2})/\Gamma(K_{\mu 2})$ with an accuracy at the % level, aiming at finding evidence of deviations from the SM prediction induced by lepton-flavor violation NP effects.

1 Introduction

New precise measurements of $K \to l\nu_l(\gamma)$ (K_{l2}) and $K \to \pi l\nu_l(\gamma)$ (K_{l3}) decays can possibly shed light on new physics (NP). The first indication of the need of improving the present knowledge in this field was given by the 2004 version of the PDG: a deviation from unitarity of the CKM matrix was observed in the first row, amounting to more than two standard deviations [1],

$$\Delta = 1 - V_{ud}^2 - V_{us}^2 - V_{ub}^2 = 0.0043(16)_{Vud}(11)_{Vus}. \quad (1)$$

This called for new precise determinations of the V_{us} parameter of the CKM matrix, traditionally extracted from K_{l3} decays using the following expression:

$$\Gamma^i(K_{e3(\gamma),\,\mu 3(\gamma)}) = |V_{us}|^2 \frac{C_i^2 G_F^2 M^5}{128\pi^3} S_{\rm EW}\, |f_+^{K^0}(0)|^2 I^i_{e3,\,\mu 3}\,(1+\delta^i_{e3,\,\mu 3}), \quad (2)$$

where i indexes $K^0 \to \pi^-$ and $K^+ \to \pi^0$ transitions for which $C_i^2 = 1$ and $1/2$, respectively, G_F is the Fermi constant, M is the appropriate kaon mass, and $S_{\rm EW}$ is a universal short-distance electroweak correction [2]. The δ^i term accounts for long-distance radiative corrections depending on the meson charges and lepton masses and, for $K^{\pm}$, for isospin-breaking effects. These corrections are presently known at the few-per-mil level [3]. The $f_+^{K^0}(0)$ form factor parametrizes the vector-current transition $K^0 \to \pi^-$ at zero momentum transfer t, while the dependence of

vector and scalar form factors on t enter into the determination of the integrals $I_{e3,\,\mu3}$ of the Dalitz-plot density over the physical region.

After four years of analysis of KLOE data, we present the most comprehensive set of results from a single experiment, including BR's for K_{e3} and $K_{\mu3}$ decays for K_L [4] and $K^{\pm}$ [5], and the BR for $K_S \to \pi e \nu$ [6,7] (unique to KLOE); form factor slopes from analysis of K_{Le3} [8] and $K_{L\mu3}$ [9]; lifetime measurements for K_L [10] and $K^{\pm}$ [11]; the K^0 mass [12]. Using the K_S lifetime from PDG [13] as the only input other than KLOE measurements, we obtain five results for the product $f_+(0)|V_{us}|$ [14], as shown in table 1. The average of these has been obtained taking all correlations into account and it is $f_+(0) \times |V_{us}| = 0.2157(6)$. As a comparison, using data from KLOE, KTeV, NA48, and ISTRA+ experiments, the world average [15] is 0.2166(5). From the KLOE result and using $f_+(0) = 0.9644(49)$ from the UKQCD/RBC collaboration [16], we obtain

$$|V_{us}| = 0.2237(13). \tag{3}$$

Using the world average [17] $V_{ud} = 0.97418(26)$ from $0^+ \to 0^+$ nuclear β decays, CKM unitarity can be seen to be satisfied: $\Delta = 9(8) \times 10^{-4}$.

KLOE has provided the most precise determination of the $K_{\mu2}$ BR [18], which can be linked to the ratio V_{us}/V_{ud} via the following relation [19]:

$$\frac{\Gamma(K \to \mu\nu)}{\Gamma(\pi \to \mu\nu)} = \frac{m_K \left(1 - m_\mu^2/m_K^2\right)^2}{m_\pi \left(1 - m_\mu^2/m_\pi^2\right)^2} \left|\frac{V_{us}}{V_{ud}}\right|^2 \frac{f_K^2}{f_\pi^2} C.$$

The theoretical inputs are the form-factor ratio f_K/f_π and the radiative corrections described by the factor C. We use $f_K/f_\pi = 1.189(7)$ from lattice calculations [20] and $C = 0.9930(35)$ [19], thus obtaining

$$|V_{us}/V_{ud}| = 0.2326(15). \tag{4}$$

From the KLOE results of Eqs. 3 and 4, and from the world-average value of V_{ud}, a combined fit to V_{us} and V_{ud} has been done. The result is shown in left panel of Fig. 1: the fit χ^2 is 2.34 for one degree of freedom (13% probability) and the results are: $|V_{us}| = 0.2249(10)$ and $|V_{ud}| = 0.97417(26)$, with a correlation of 3%. From these, not only can we now state that the CKM unitary holds to within 10^{-3}, $\Delta = 0.0004 \pm 0.0005_{Vud} \pm 0.0004_{Vus}$, but we can obtain severe constraints for many NP models.

1.1 Unitarity and coupling-universality tests

In the SM, unitarity of the weak couplings and gauge universality dictate:

$$G_{\rm F}^2 \left(|V_{ud}|^2 + |V_{us}|^2\right) = G_\mu^2 \ \left(V_{ub}^2 \text{ negligible}\right), \tag{5}$$

where G_μ^2 is the decay constant obtained from the measurement of the μ lifetime [21]. The above measurement of V_{us}^2 from KLOE inputs provides relevant tests for possible breaking of the CKM unitarity ($\Delta \neq 0$) and/or of the coupling universality ($G_F \neq G_\mu$). This can happen in some NP scenarios, some example of which we discuss below.

NP might lead to exotic and still unobserved μ decays contributing to the μ lifetime. The resulting total BR for μ exotic modes equals the unitarity violation Δ. Some of these modes, such as $\mu^+ \to e^+ \overline{\nu}_e \nu_\mu$, are at present constrained to be less than $\sim 1\%$, so that information from unitarity improves on that from direct searches by more than a factor of 10 [22,23].

The existence of additional heavy Z bosons would influence unitarity at the loop level entering in muon and charged current semileptonic decays differently [24]: $\Delta = -0.01\lambda \ln[r_Z^2/(r_Z^2 - 1)]$, where $r_Z = m_{Z'}/m_W$ and λ is a model-dependent constant of order 1. In the case of $SO(10)$

grand unification, $\lambda \sim 1.9$ and a unitarity test from KLOE results yields $M_{Z'} > 750$ GeV at 95% of CL. In non-universal gauge interaction models, a tree-level contribution from Z' bosons appears, so that the unitarity test is sensitive to even larger masses [25].

In supersymmetric extensions of the SM (SUSY), loops affect muon and semileptonic decays differently. Unitarity can constrain SUSY up to mass scales of the order of 0.5 TeV, depending on the extent of cancellation between squark and slepton effects [26].

Measurements of K_{l2} widths can be linked to new physics effects, too. The ratio of $K_{\mu 2}$ to $\pi_{\mu 2}$ decay widths might accept NP contributions from charged Higgs exchange [27,28] in supersymmetric extensions of the SM with two Higgs doublets. In this scenario, the ratio V_{us}/V_{ud} extracted from $K_{\mu 2}$, $\pi_{\mu 2}$ should differ from that extracted from K_{l3} and superallowed Fermi transitions ("0^+"):

$$\left|\frac{V_{us}(K_{l2})V_{ud}(0^+)}{V_{us}(K_{l3})V_{ud}(\pi_{l2})}\right| = \left|1 - \frac{m_K^2(m_s - m_d)\tan^2\beta}{M_H^2 m_s(1+\epsilon_0\tan\beta)}\right|,$$

where $\tan\beta$ is the ratio of up- and down-Higgs vacuum expectation values, M_H is the charged Higgs mass, and $\epsilon_0 \sim 0.01$ [29]. The KLOE result of Eq. 4 can be translated into an exclusion plot in the plane $\tan\beta$ vs M_H (see right panel of Fig. 1), showing that this analysis is complementary to and competitive with that [28] using the average $\mathrm{BR}(B \to \tau\nu) = 1.73(35) \times 10^{-4}$ of Babar and Belle measurements [30].

Mode	$f_+ \times \lvert V_{us}\rvert$	Error,%
K_{Le3}	0.2155(7)	0.3
$K_{L\mu 3}$	0.2167(9)	0.4
K_{Se3}	0.2153(14)	0.7
$K^{\pm}_{e3}$	0.2152(13)	0.6
$K^{\pm}_{\mu 3}$	0.2132(15)	0.7

Table 1: Five determinations of $f_+ \times |V_{us}|$ using the K_S lifetime (from PDG) as the only input other than KLOE measurements.

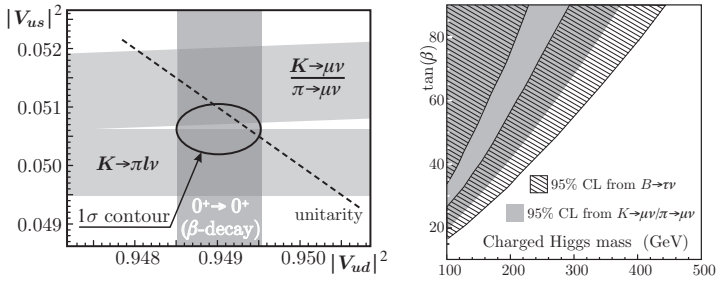

Figure 1: Left: The 1-σ fit result to V_{ud} and V_{us} is shown by the solid line ellipse, in agreement with the unitarity bound shown by the dashed line. Right: Excluded regions from analysis of decays $K \to \mu\nu$ (filled area) and $B \to \tau\nu$ (hatched area).

1.2 Test of lepton-flavor violation

A significant effort has been devoted along the years to isolate signals from lepton flavor violating (LFV) transitions, which are forbidden or ultra-rare in the Standard Model (SM). The sensitivity to decays such as $\mu \to e\gamma$, $\mu \to eee$, $K_L \to \mu e(+\pi^0\text{'s})$, and others roughly improved by two orders of magnitude for each decade [31]. No signal has been observed, thus ruling out SM extensions with LFV amplitudes with mediator masses below ~ 100 TeV.

These results allowed the focus to be put on the detection of NP-LFV effects in loop amplitudes, by studying specific processes suppressed in the SM. In this field, a strong interest for a new measurement of the ratio $R_K = \Gamma(K \to e\nu)/\Gamma(K \to \mu\nu)$ has recently arisen, triggered by the work of Ref. [32]. The SM prediction of R_K benefits from cancellation of hadronic uncertainties to a large extent and therefore can be calculated with high precision. Including radiative corrections, the total uncertainty is less than 0.5 per mil [33]:

$$R_K = (2.477 \pm 0.001) \times 10^{-5}. \quad (6)$$

Since the electronic channel is helicity-suppressed by the $V - A$ structure of the charged weak current, R_K can receive contributions from physics beyond the SM, for example from multi-Higgs

effects inducing an effective pseudoscalar interaction. It has been shown in Ref.[32] that deviations from the SM of up to few percent on R_K are quite possible in minimal supersymmetric extensions of the SM and in particular should be dominated by lepton-flavor violating contributions with tauonic neutrinos emitted in the electron channel:

$$R_K = R_K^{\mathrm{SM}} \times \left[1 + \left(\frac{m_K^4}{m_H^4}\right)\left(\frac{m_\tau^2}{m_e^2}\right)\left|\Delta_R^{31}\right|^2 \tan^6\beta\right], \tag{7}$$

where M_H is the charged-Higgs mass, Δ_R^{31} is the effective e-τ coupling constant depending on MSSM parameters, and $\tan\beta$ is the ratio of the two vacuum expectation values. Note that the pseudoscalar constant f_K cancels in R_K^{SM}.

In order to compare with the SM prediction at this level of accuracy, one has to treat carefully the effect of radiative corrections, which contribute to nearly half the $K_{e2\gamma}$ width. In particular, the SM prediction of Eq. 7 is made considering all photons emitted by the process of internal bremsstrahlung (IB) while ignoring any contribution from structure-dependent direct emission (DE). Of course both processes contribute, so in the analysis DE is considered as a background which can be distinguished from the IB width by means of a different photon energy spectrum.

Two experiments are participating in the challenge to push the error on R_K from the present 6% down to less than 1%. In 2007, KLOE and NA48/2 announced preliminary results[34] with errors ranging from 2% to 3%. Moreover, the new NA62 collaboration collected more than 100 000 K_{e2} events in a dedicated run of the NA48 detector, aiming at reaching an accuracy of few per mil on R_K[35].

2 Measuring R_K at KLOE

DAΦNE, the Frascati ϕ factory, is an e^+e^- collider working at $\sqrt{s} \sim m_\phi \sim 1.02$ GeV. ϕ mesons are produced, essentially at rest, with a visible cross section of ~ 3.1 μb and decay into K^+K^- pairs with a BR of $\sim 49\%$.

Kaons get a momentum of ~ 100 MeV/c which translates into a low speed, $\beta_K \sim 0.2$. K^+ and K^- decay with a mean length of $\lambda_\pm \sim 90$ cm and can be distinguished from their decays in flight to one of the two-body final states $\mu\nu$ or $\pi\pi^0$.

The kaon pairs from ϕ decay are produced in a pure $J^{PC} = 1^{--}$ quantum state, so that observation of a K^+ in an event signals, or tags, the presence of a K^- and vice versa; highly pure and nearly monochromatic $K^\pm$ beams can thus be obtained and exploited to achieve high precision in the measurement of absolute BR's.

The analysis of kaon decays is performed with the KLOE detector, consisting essentially of a drift chamber, DCH, surrounded by an electromagnetic calorimeter, EMC. A superconducting coil provides a 0.52 T magnetic field. The DCH[36] is a cylinder of 4 m in diameter and 3.3 m in length, which constitutes a fiducial volume for $K^\pm$ decays extending for $\sim 1\lambda_\pm$. The momentum resolution for tracks at large polar angle is $\sigma_p/p \leq 0.4\%$. The c.m. momenta reconstructed from identification of 1-prong $K^\pm \to \mu\nu, \pi\pi^0$ decay vertices in the DC peak around the expected values with a resolution of 1–1.5 MeV, thus allowing clean and efficient $K^\mp$ tagging.

The EMC is a lead/scintillating-fiber sampling calorimeter[37] consisting of a barrel and two endcaps, with good energy resolution, $\sigma_E/E \sim 5.7\%/\sqrt{\mathrm{E(GeV)}}$, and excellent time resolution, $\sigma_T = 54$ ps$/\sqrt{\mathrm{E(GeV)}} \oplus 50$ ps.

In early 2006, the KLOE experiment completed data taking, having collected ~ 2.5 fb^{-1} of integrated luminosity at the ϕ peak, corresponding to $\sim$3.6 billion K^+K^- pairs. Using the present KLOE dataset, a measurement of R_K with an accuracy of about 1 % has been performed.

Given the $K^\pm$ decay length of $\sim$90 cm, the selection of one-prong $K^\pm$ decays in the DC required to tag $K^\mp$ has an efficiency smaller than 50%. In order to keep the statistical uncertainty on the number of $K \to e\nu$ counts below 1%, a "direct search" for $K \to e\nu$ and $K \to \mu\nu$ decays

is performed, without tagging. Since the wanted observable is a ratio of BR's for two channels with similar topology and kinematics, one expects to benefit from some cancellation of the uncertainties on tracking, vertexing, and kinematic identification efficiencies. Small deviations in the efficiency due to the different masses of e's and μ's will be evaluated using MC.

Selection starts by requiring a kaon track decaying in a DC fiducial volume (FV) with laboratory momentum between 70 and 130 MeV, and a secondary track of relatively high momentum (above 180 MeV). The FV is defined as a cylinder parallel to the beam axis with length of 80 cm, and inner and outer radii of 40 and 150 cm, respectively. Quality cuts are applied to ensure good track fits.

A powerful kinematic variable used to distinguish $K \to e\nu$ and $K \to \mu\nu$ decays from the background is calculated from the track momenta of the kaon and the secondary particle: assuming $M_\nu = 0$, the squared mass of the secondary particle ($M^2_{\rm lep}$) is evaluated. The distribution of $M^2_{\rm lep}$ is shown in Fig. 2 for MC events before and after quality cuts are applied. The selection applied is enough for clean identification of a $K \to \mu\nu$ sample, while further rejection is needed in order to identify $K \to e\nu$ events: the background, which is dominated by badly reconstructed $K \to \mu\nu$ events, is ∼10 times more frequent than the signal in the region around M^2_e.

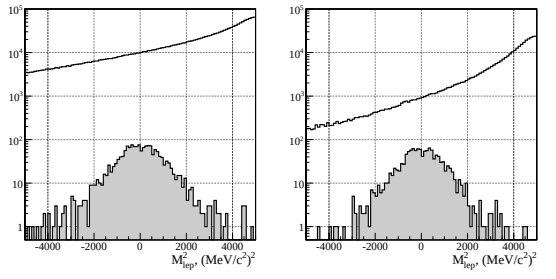

Figure 2: MC distribution of $M^2_{\rm lep}$ before (left) and after (right) quality cuts are applied. Shaded histogram: $K \to e\nu$ events. Open histograms: background. In MC, R_K is set to the SM value.

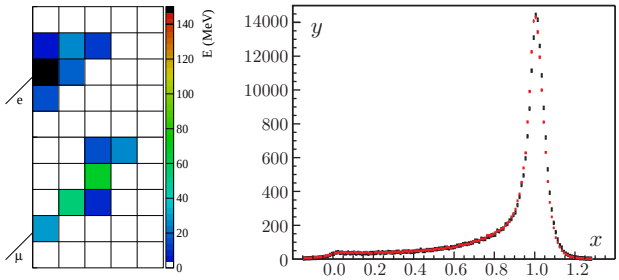

Figure 3: Left: cell distribution for 200 MeV e (top) and μ (bottom) from two selected events from $K_L \to \pi\ell\nu$. Right: Distribution of NN output, NN, for electrons of a $K_L \to \pi e\nu$ sample from data (black histogram) and MC (red histogram).

Information from the EMC is used to improve background rejection. To this purpose, we extrapolate the secondary track to the EMC surface and associate it to a nearby EMC cluster. For electrons, the associated cluster is close to the EMC surface and the cluster energy $E_{\rm cl}$ is a measurement of the particle momentum $p_{\rm ext}$, so that $E_{\rm cl}/p_{\rm ext}$ peaks around 1. For muons, clusters tend to be more in depth in the EMC and $E_{\rm cl}/p_{\rm ext}$ tends to be smaller than 1, since only the kinetic energy is visible in the EMC. Electron clusters can also be distinguished from μ (or π) clusters, since electrons shower and deposit their energy mainly in the first plane of EMC, while muons behave like minimum ionizing particles in the first plane and deposit a sizable fraction of their kinetic energy from the third plane onward, when they are slowed down to rest (Bragg's peak), see left panel of Fig. 3. Particle identification has been therefore based on the asymmetry of energy deposits between the first and the next-to-first planes, on the spread of energy deposits on each plane, on the position of the plane with the maximum energy, and on the asymmetry of energy deposits between the last and the next-to-last planes. All information are combined with neural network (NN) trained on $K_L \to \pi\ell\nu$ data, taking into account variations of the EMC response with momentum and impact angle on the calorimeter. The distribution of the NN output, NN, for an independent $K_L \to \pi e\nu$ sample is shown in the right panel of Fig. 3 for data and Monte Carlo (MC). Additional separation has been obtained using time of flight information.

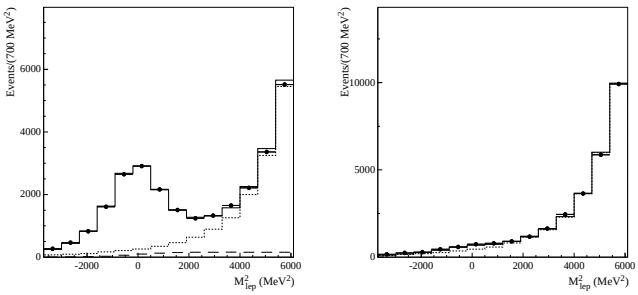

Figure 4: Fit projections onto the $M^2_{\rm lep}$ axis for two slices in NN output, NN > 0.98 and NN < 0.98, giving enhanced values of signal and background contributions, respectively.

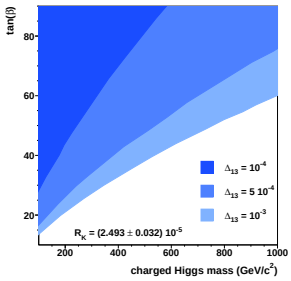

Figure 5: 95%-CL excluded regions in the plane $\tan\beta$–charged Higgs mass for $\Delta^{31}_R = 10^{-4},\ 5\times10^{-3},\ 10^{-3}$.

The number of $K \to e\nu(\gamma)$ is determined with a binned likelihood fit to the two-dimensional NN vs $M^2_{\rm lep}$ distribution. Distribution shapes for signal and $K_{\mu 2}$ background, other sources being negligible, are taken from MC; the normalization factors for the two components are the only fit parameters. In the fit region, a small fraction of $K \to e\nu(\gamma)$ events is due to the direct-emission structure-dependent component (DE): the value of this contamination, $f_{\rm SD}$, is fixed in the fit to the expectation from simulation.This assumption has been evaluated by performing a dedicated measurement of SD, which yielded as a by-product a determination of f_{SD} with a 4% accuracy. This implies a systematic error on K_{e2} counts of 0.2%, as obtained by repeating the fit with values of $f_{\rm SD}$ varied within its uncertainty.

In the fit region, we count 7064±102 $K^+ \to e^+\nu(\gamma)$ and 6750±101 $K^- \to e^-\bar\nu(\gamma)$ events. Fig. 4 shows the sum of fit results for K^+ and K^- projected onto the $M^2_{\rm lep}$ axis in a signal- (NN > 0.98) and a background- (NN < 0.98) enhanced region.

To assess the uncertainty on the R_K measurement arising from limited knowledge of the momentum resolution we have examined the agreement between the $M^2_{\rm lep}$ distributions for data and MC in the $K_{\mu 2}$ region. For the NN distribution, the EMC response at the cell level has been tuned by comparing data and MC samples. In order to evaluate the systematic error associated with these procedures, we studied the result variation with different fit range values, corresponding to a change for the overall K_{e2} purity from $\sim 75\%$ to $\sim 10\%$. The results are stable within statistical fluctuations. A systematic uncertainty of 0.3% for R_K is derived "à la PDG" [13] by scaling the uncorrelated errors so that the reduced χ^2 value of results is 1.

The number of $K_{\mu 2}$ events in the same data set is extracted from a fit to the $M^2_{\rm lep}$ distribution. The fraction of background events under the muon peak is estimated from MC to be $< 0.1\%$. We count 2.878×10^8 (2.742×10^8) $K^+_{\mu 2}$ ($K^-_{\mu 2}$) events. Difference in K^+ and K^- counting is ascribed to K^- nuclear interactions in the material traversed.

The ratio of K_{e2} to $K_{\mu 2}$ efficiency is evaluated with MC and corrected for data-to-MC ratios using control samples. To check the corrections applied we also measured $R_3 = {\rm BR}(K_{e3})/{\rm BR}(K_{\mu 3})$, in the same data sample and by using the same methods for the evaluation of the efficiency as for the R_K analysis. We found $R_3 = 1.507(5)$ and $R_3 = 1.510(6)$, for K^+ and K^- respectively. These are in agreement within a remarkable accuracy with the expectation [15] from world-average form-factor slope measurements, $R_3 = 1.506(3)$.

3 R_K result and interpretation

The final result is $R_K = (2.493 \pm 0.025 \pm 0.019)\times10^{-5}$. The 1.1% fractional statistical error has contributions from signal count fluctuation (0.85%) and background subtraction. The 0.8%

systematic error has a relevant contribution (0.6%) from the statistics of the control samples used to evaluate corrections to the MC. The result does not depend on K charge: quoting olny the uncorrelated errors, $R_K(K^+) = 2.496(37)10^{-5}$ and $R_K(K^-) = 2.490(38)10^{-5}$.

The result in agreement with SM prediction of Eq. 6. Including the new KLOE result, the world average reaches an accuracy at the % level: $R_K = 2.468(25) \times 10^{-5}$. In the framework of MSSM with LFV couplings, the R_K value can be used to set constraints in the space of relevant paremeters (see eq. 7). The regions excluded at 95% C.L. in the plane $\tan\beta$–charged Higgs mass are shown in Fig. 5 for different values of the effective LFV coupling Δ_R^{31}.

1. Particle Data Group, Phys. Lett. B **592**, 1 (2004).
2. A. Sirlin, Rev. Mod. Phys. **50**, 573 (1978); Nucl. Phys. B **196**, 83 (1982).
3. V. Cirigliano *et al.* Eur. Phys. J. C **23**, 121 (2002).
4. KLOE Coll., Phys. Lett. B **632**, 43 (2006).
5. KLOE Coll., JHEP **0802**, 098 (2008).
6. KLOE Coll., Phys. Lett. B **636**, 173 (2006).
7. KLOE Coll., Eur. Phys. J. C **48**, 767 (2006).
8. KLOE Coll., Phys. Lett. B **636**, 166 (2006).
9. KLOE Coll., JHEP **0712**, 105 (2008) and arXiv:0707.4631 (2007).
10. KLOE Coll., Phys. Lett. B **626**, 15 (2005).
11. KLOE Coll., JHEP **0801**, 073 (2008).
12. KLOE Coll., JHEP **0712**, 073 (2007).
13. Particle Data Group, Phys. Lett. B **667**, 1 (2008).
14. KLOE Coll., JHEP **0804**, 059 (2008).
15. FlaviaNet Working Group on Kaon Decays, arXiv:0801.1817.
16. RBC/UKQCD Coll., arXiv:0710.5136 (2007).
17. I. S. Towner and J. C. Hardy, arXiv:0710.3181 (2007)
18. KLOE Coll., Phys. Lett. B **632**, 76 (2006).
19. W. J. Marciano, Phys. Rev. Lett. **93**, 231803 (2004).
20. HPQCD/UKQCD Coll., arXiv:0706.1726 (2007).
21. MuLan Coll., Phys. Rev. Lett. **99**, 032001 (2007), arXiv:0704.1981.
22. Review by W. J. Marciano and E. Blucher, pages 733-737 of Ref. [13].
23. W. J. Marciano, PoS **KAON**, 003 (2007).
24. W. Marciano and A. Sirlin, Phys. Rev. **D35**, 1672 (1987).
25. K. Y. Lee, Phys. Rev. **D76**, 117702 (2007).
26. R. Barbieri *et al.*, Phys. Lett. **B156**, 348 (1985); K. Hagiwara *et al.*, Phys. Rev. Lett. **75**, 3605 (1995); A. Kurylov and M. Ramsey-Musolf, Phys. Rev. Lett. **88**, 071804 (2000).
27. W. S. Hou, Phys. Rev. D **48**, 2342 (1992).
28. G. Isidori and P. Paradisi, Phys. Lett. B **639**, 499 (2006).
29. G. Isidori and A. Retico, JHEP **11**, 001 (2001).
30. Belle Coll., Phys. Rev. Lett. **97**, 251802 (2006); Babar Coll., Phys. Rev. **D76**, 052002 (2007). For Belle and Babar updates, see A. Bozek and E. Baracchini contributions in the 2009 edition of Rencontrès de Moriond EW.
31. L. G. Landsberg, Phys. Atom. Nucl. **68**, 1190 (2005) [arXiv:hep-ph/0410261].
32. A. Masiero, P. Paradisi, and R. Petronzio, Phys. Rev. D **74**, 011701 (2006).
33. V. Cirigliano and I. Rosell, arXiv:0707.4464 (2007).
34. A. Sibidanov [KLOE collab.], arXiv:0707.4623 (2007); L. Fiorini [NA48], Nucl. Phys. Proc. Suppl. **169**, 205 (2007); V. Kozhuharov [NA48], PoS **KAON**, 049 (2007).
35. See A. Winhart contribution in the 2009 edition of Rencontrès de Moriond EW.
36. KLOE Coll., Nucl. Instrum. Methods A **488**, 51 (2002).
37. KLOE Coll., Nucl. Instrum. Methods A **482**, 364 (2002).